

A Data-Driven fMRI Neuronal Activation Analysis Method Using Temporal Clustering Technique and an Adaptive Voxel Selection Criterion

Sarah Lee*, Fernando Zelaya†, Stephanie A. Amiel‡ and Michael J. Brammer*

Abstract—Functional magnetic resonance imaging (fMRI) is one of the most widely used methods to study neuronal activity in human brain. A data-driven analysis method is proposed for studying brain responses when the information for predicting their onset or duration is unavailable. The method is suitable for experiments involving a single event or non-repetitive multiple events. It is built upon the pre-existing temporal clustering analysis techniques with additional features that make use of the signal changes of neighbouring voxels to ensure that the selected voxels for response detection are those which are most likely to have been activated by the stimuli. For method validation, eight sets of fMRI data from three different kinds of sensory experiments are applied. The results demonstrate that our method is able to detect the time bins during which the stimuli were administered and the identified voxels correspond to the brain areas, which are typically activated in this kind of experiment. Moreover, in these eight sets of data, the accuracy of stimulation response detection is 75% in comparison to 58.33% without the selection criterion.

Keywords: magnetic resonance imaging, image analysis, brain digital filters, signal analysis

1 Introduction

Over the past decade, fMRI (functional magnetic resonance imaging) has been one of the most widely used methods for studying brain activity during experiments

*The authors would like to thank the Wellcome Trust for the project funding. S. Lee and M.J. Brammer are with Brain Image Analysis Unit, Institute of Psychiatry, King's College London, SE8 8AF United Kingdom *sarah.lee at iop.kcl.ac.uk*, *m.brammer at iop.kcl.ac.uk*

†F. Zelaya is with Institute of Psychiatry, King's College London, SE8 8AF United Kingdom *f.zelaya at iop.kcl.ac.uk*

‡S. Lee and S.A. Amiel are with Diabetes Research Group, School of Medicine at King's College Hospital, King's College London. SE5 9PJ United Kingdom *stephanie.amiel at kcl.ac.uk*

which are designed to investigate brain function [10]. Detection of brain activation is carried out by analysing the blood oxygenation level dependent (BOLD) time series, at each voxel in the four-dimensional (4D) fMRI data: $X \times Y \times T \times S$, where X and Y are the number of voxels in the x and y axes, T is the number of volumes and S is the number of slices acquired. The voxels "activated" in a particular experiment are then indicated on an activation map.

The methods for obtaining activation maps can be broadly divided into two categories: model-driven methods and data-driven methods [10]. In model-driven methods, the temporal response to the stimulation is estimated, e.g., the convolution of a stimulus function with the haemodynamic response function. The model is then fitted to the time series of each voxel and the significance of the resulting fits is assessed to identify "activated" voxels. The most common approach is based on the general linear model (GLM) [10]. In data-driven methods, such a model is unavailable, and brain activation is detected using only information within fMRI signal.

In this category, techniques such as independent component analysis (ICA) [17] and wavelet transformation [4] have been used to extract the main components of response from the fMRI time series. Recently, a number of temporal clustering analysis (TCA) techniques [9, 12, 13, 14, 15, 20] have been suggested. These are designed to detect the brain responses from the fMRI data involving single event or non-repetitive multiple events. In the original OTCA [15], modified TCA (MTCA) [20] and iterative MTCA (ITCA) [9], one slice of fMRI data is taken to locate the temporal maximum of the time series of each voxel and the time point at which the highest number of voxels reached their maxima is the main parameter of interest. OTCA used the average signal intensity as baseline; MTCA eliminated this procedure; ITCA was proposed to detect multiple peaks: TCA was used to detect the first peak and the associated data points

were removed before the TCA was applied again to detect the second peak. The procedure was repeated n_{peak} times, where n_{peak} was the number of expected peaks. In [12], the spatial information of the detected voxels within a slice was also taken into consideration by introducing a 3×3 neighbourhood test to the temporal maximum voxels, since the physiologically plausible brain activation seldom occur in single isolated voxels. The idea was extended into all slices, so that the whole brain data were taken into consideration [13]. The response to the stimulation was determined by the time bins with the highest numbers of detected voxels. Furthermore, the neighbourhood test was extended into three dimensions ($3 \times 3 \times 3$), in order to include the neighbouring voxels in adjacent slices [14].

In this paper, we propose a new voxel selection criterion, which examines the mean squared error in the percentage signal change between the detected voxel and all the possible combinations of its neighbouring voxels, which also reached their maxima at the same time bin, in a 3×3 neighbourhood. The proposed method is applied to eight sets of fMRI data of three different kinds of sensory experiments as validation.

2 Method

The proposed method can be broken down into three stages. Stage 1: Pre-processing of the fMRI data including head motion correction [3] and computation of a brain tissue mask [19]. Filtering processes are then applied to eliminate low- and high-frequency noise and the 4D fMRI data are reduced to a 2D data set using TCA techniques [9, 15, 20]: the data are processed slice by slice and only the time series of the voxels inside the brain mask are placed row by row in a 2D matrix. Stage 2: Determining the temporal maximum of each voxel and an adaptive voxel selection is applied to find the voxels which are most likely to be activated by the stimulation. Stage 3: The brain response is detected using the information obtained in Stage 2 throughout the whole brain. The details can be found in the following sub-sections.

2.1 Stage 1: Pre-processing and Filtering

In the pre-processing step, the fMRI data are first corrected for head motion using in-house software [3] and a brain mask is obtained using FSL Brain Extraction Tool [19]. The 4D fMRI data set ($X \times Y \times T \times S$, where X and Y are the number of voxels in the x and y axes, T is the number of volumes and S is the number of slices acquired during the experiment) is processed slice by slice, i.e., the data dimension is first reduced to 3 ($X \times Y \times T$) [8]. For each slice, the TCA data representation techniques [9, 15, 20] are applied. The 3D data are reduced to 2D

by placing the time series of the voxels inside the brain mask row by row in a 2D matrix: $\underline{D}_{ori,s}$, $s = 0, \dots, S-1$. The matrix $\underline{D}_{ori,s}$ of size $N_s \times T$, where N_s is the number of voxels inside the brain mask for slice s , allows us to observe the changes in the time series of every voxel within the brain mask.

The data for each time series in $\underline{D}_{ori,s}$, $s = 0, \dots, S-1$ are converted from signal intensity to percentage signal change to form matrix $\underline{D}_{psc,s}$ of size $N_s \times T$, $s = 0, \dots, S-1$ to permit comparison of signal changes between voxels.

In order to eliminate temporal spikes, a 5-point moving average filter is applied to the time series in $\underline{D}_{psc,s}$, followed by a bandpass filtering process to eliminate high-frequency noise and low-frequency noise caused by slowly varying unwanted signals, such as heartbeat, breathing or scanner-related drifts [10]. The matrix with time series after filtering processes is regarded as $\underline{D}_{filtered,s}$ of size $N_s \times T$.

The response detection is reinforced by temporal averaging [12, 13, 14], which is carried out by taking the mean of the percentage changes in signal in a block of n time points for each time series in $\underline{D}_{filtered,s}$, since the activation in voxels throughout the brain to a block to stimuli may not happen at the same time point. The unit of the time series is now time bin instead of time point and the data matrix now becomes $\underline{D}_{processed,s}$ of size $N_s \times (T/n)$.

2.2 Stage 2: Voxel Selection

The goal of this stage is to select the voxels which are most likely to be plausibly activated by the stimulation. The candidate voxels are obtained by applying the detection of the temporal maximum in TCA methods [9, 15, 20], i.e., to determine the time point at which most voxels reach their maxima.

In this work, voxels in the 3×3 neighbourhood of every detected maximum voxel are examined using the mean squared error (MSE) between their percentage signal changes and the percentage change of the maximum voxel. This is called ‘adaptive voxel selection’ since all the possible combinations of these eight neighbouring voxels are explored.

If a voxel with its temporal maximum at time bin τ is at co-ordinate $(m_{(s,x_\alpha)}, m_{(s,y_\alpha)})$, its candidate neighbouring voxels for the selection are the ones which also reach their maxima at the same time bin within the range $[m_{(s,x_\alpha)} - 1 : m_{(s,x_\alpha)} + 1, m_{(s,y_\alpha)} - 1 : m_{(s,y_\alpha)} + 1]$. Voxels with more than 50% of their neighbouring voxels also reach their maxima at the same time bin are taken into consideration. The ‘50%’ measure is introduced, in or-

der to eliminate the maxima caused by artefacts. The percentage signal change of the valid neighbouring voxels at this time bin are placed in a vector, \underline{V} . All the possible voxel combinations are found, i.e., ${}_L C_k$, where L is the length of \underline{V} and $k = 1, \dots, L$. The MSE between each possible combination and the maximum voxel is computed. The chosen MSE should be as small as possible whereas the number of neighbouring voxels to be included should be as large as possible. We search for the minimum MSE and obtain the neighbouring voxel combination that contains the maximum number of voxels and within +10% of the minimum MSE. The number of detected voxels is recorded for every slice at every time bin in matrix \underline{F} of size $S \times (T/n)$.

2.3 Stage 3: Stimulus Response Detection

The output of Stage 2, \underline{F} is used for stimulus response detection. The matrix is summed column wise, in order to find the time bins with the highest numbers of detected voxels. The time bins with the four highest numbers of detected voxels are recorded and their activation maps are generated by colouring the corresponding voxels red. If the responses to the stimuli are the largest signals in the time series in all slices, the number of selected time bins should have been the same as the number of stimuli in the experiments. However, it was observed in our data that the responses to the stimuli might not always be the greatest when all the slices are taken into account. Other sources of physiological or external noise, e.g., [7] could also cause a large number of voxels to reach their maxima at the same time. In order to allow some flexibility, four time bins with the highest number of detected voxels are considered.

3 fMRI Data and Parameters

The proposed method can be applied to any single-event or non-repetitive multi-event experimental design. For method validation, it was applied to eight sets of fMRI data from three different kinds of sensory experiments, since the brain regions activated in these kinds of experiments have been characterised extensively. The data were acquired on a 1.5 Tesla GE scanner at the Centre for Neuroimaging Sciences, Institute of Psychiatry, King's College London.

Visual Experiment

A period of 8-Hz flickering checkerboard visual stimuli was presented to a healthy subject between 60-120 seconds (s) after the start of the experiment, which lasted for a total of 300s. 150 volumes of 20 axial slices were acquired with a repetition time (TR) equal to 2s. Each slice contained 64×64 voxels and its voxel dimensions

were $3.75\text{mm} \times 3.75\text{mm} \times 5.5\text{mm}$. The four sets of data for validation were labelled: VIS1, VIS2, VIS3 and VIS4.

Visual and Auditory Experiment

In addition to the aforementioned visual stimuli, a block of auditory stimuli occurred between 210-274s. The experiment, again, lasted 300s and 150 volumes of 25 axial slices with TR=2s were acquired. The voxel dimensions remained the same. One set of data was obtained: VIS-AUD.

Visual and Motor Experiment

The visual stimuli were the same as in VIS1-4 and VIS-AUD. Motor stimuli consisting of squeezing a rubber ball in the right hand at a rate of once every two seconds were administered between 240-300s in a 360s long experiment on a healthy subject with TR=2s. 180 volumes of 20 axial slices were acquired and the voxel dimensions remained the same. Three sets of data used are labelled: VIS-MOT1, VIS-MOT2 and VIS-MOT3.

Parameters used in the proposed method: a 5-point moving average filter, a bandpass filter with passband between 1/80 to 1/40 Hz. For the stimuli used in this test are bin size, i.e., n , of 5 points for starting value.

4 Results and Discussion

The stimulus detection results obtained with the proposed method can be found in Table 1, where the time bins corresponding to the four highest numbers of detected voxels are given. When the detected time bin falls into the period during which the stimuli were applied and the voxels contributed to this detection were in the brain areas which were typically found activated during these kinds of sensory experiments, a record is made in the table: 'A' for auditory cortex for auditory stimuli (e.g., [1, 2, 11]), 'M' for the supplementary motor area (SMA) and motor areas for the motor stimuli [6], and 'V' for the primary and extrastriate visual areas for visual stimuli [5, 6, 10]. The activation maps of five most representative slices are shown for the cases when the stimulation responses were detected and the figure number is given in superscript in Table 1.

Our method detected the single block of visual stimuli in three out of the four visual data sets studied. The time bins detected that fall into the period during which the visual stimuli were applied were 70-80s for VIS1-3 and Fig. 1, 3, and 5 show that the voxels contributed to the temporal detection of the responses are distributed in the primary and extrastriate visual areas. Fig. 2, 4, and 6 are the average time series extracted from the detected voxels corresponding to Fig. 1, 3, and 5 respectively. The rest of the detected time bins did not correlate with the

stimuli.

The response to both visual and auditory stimuli were detected in VIS-AUD. The time bin with the third highest number of detected voxels was 220-230, which was right after a block of auditory stimuli was applied and the voxels that contributed were in the area of auditory cortex (Fig. 7) and the time series extracted from these voxels are shown in Fig. 8, which shows a clear peak during 220-230s and the characteristics of the fMRI time series of activation [10]. The time bin with the fourth highest number of detected voxels was 70-80s, during the period when a block of visual stimuli was applied and the voxels identified were in the primary and extrastriate visual areas as shown in Fig. 9 and the time series extracted from these voxels is shown in Fig. 10. The time bins found with the highest and second highest detected voxels were not correlate with the stimuli.

In three sets of VIS-MOT data, the responses to both visual and motor stimuli were detected in VIS-MOT1 during the period when the stimuli were applied and the voxels that contributed are shown in red in Fig. 11 and 13 respectively. Their time series were also extracted and can be found in Fig. 12 and 14. The responses to the visual stimuli were found in the time bin with the highest number of detected voxels in VIS-MOT2 as in Fig. 15 with their time series plot in Fig. 16. The responses to the motor stimuli were found in the time bin with the third highest number of detected voxels in VIS-MOT3 right after the stimuli were administered and the activated voxels are shown in Fig. 17 and their time series in Fig. 18.

In order to see the difference in response detection with and without the adaptive selection criterion, the same procedure but without the adaptive selection criterion was applied to the same sets of data, i.e., at each time bin, all the voxels that reached their maxima in all slices were counted for the brain response detection. The time bins detected and their spatial information are given in Table 2. In comparison to the results from the proposed method, 7 out of 12 stimuli in all experiments (58.33%) were detected in the method without the adaptive selection criterion and 9 out of 12 (75%) were detected in the method with the adaptive selection criterion. In addition, the selection criterion was able to eliminate the voxels which were unlikely to have reached their maxima by the stimulation. Two examples were taken from VIS1 and VIS-MOT1. In Fig. 19, the detected voxels were shown when the time bin was 70-80s for VIS1. In Fig. 20, the detected voxels were shown for the same time bin for VIS-MOT1. Since the detected voxels did not only appear in the areas of primary and extrastriate visual areas, this result was not classified as a successful

detection.

5 Conclusion

A data-driven fMRI analysis method is proposed based on pre-existing temporal clustering analysis techniques with a novel adaptive neighbouring voxel selection criterion to detect brain responses. For validation purpose, the method has been applied to eight sets of fMRI data from three different sensory experiments. When the fMRI time series contained the responses to the stimuli, our method was able to detect the time bins in which the stimuli were applied and the voxels found were distributed in the primary and extrastriate areas for the visual stimuli, auditory cortex for the auditory stimuli and supplementary motor area for the motor stimuli. The results obtained demonstrate that the incorporation of an 'adaptive selection criterion' has a significantly higher power of detection.

References

- [1] P. Belin, R.J. Zatorre, R. Hoge, A.C. Evans, and B. Pike, "Event-related fMRI of the auditory cortex", *NeuroImage*, Vol. 10, pp. 417-429, 1999.
- [2] D. Bilecen, E. Seifritz, K. Scheffler, J. Henning, and A.-C. Schulte, "Amplitude of the human auditory cortex: an fMRI study", *NeuroImage*, Vol. 17, No. 2, pp. 710-718, 2002.
- [3] E.T. Bullmore, M.J. Brammer, S. Rabe-Hesketh, V. Curtis, R.G. Morris, S.C.R. Williams, T. Sharma and P.K. McGuire, "Methods for diagnosis and treatment of stimulus-correlated motion in generic brain activation studies using fMRI", *Human Brain Mapping*, Vol. 7, pp. 38-48, 1999.
- [4] E.T. Bullmore, J. Fadili, V. Maxim, L. Sendur, B. Whitcher, J. Suckling, M. Brammer and M. Breakspear, "Wavelets and functional magnetic resonance imaging of the human brain", *NeuroImage*, Vol. 23, pp. S234-239, 2004.
- [5] V.D. Calhoun, T. Adali, V.B. McGinty, J.J. Pekar, T.D. Watson, and G.D. Pearlson, "fMRI activation in a visual-perception task: network of areas detected using the general linear model and independent component analysis", *NeuroImage*, Vol. 14, pp. 1080-1088, 2001.
- [6] V.D. Calhoun, T. Adali, and J.J. Pekar, "A method for comparing group fMRI data using independent component analysis: application to visual, motor and visumotor tasks", *Magnetic Resonance Imaging*, Vol. 22, pp. 1181-1191, 2004.

[7] M. De Luca, C.F. Beckmann, N. De Stefano, P.M. Matthews, and S.M. Smith, "fMRI resting state networks define distinct modes of long-distance interactions in the human brain", *NeuroImage*, Vol. 29, pp. 1359-1367, 2006.

[8] EEG/MRI Matlab Toolbox, <http://eeg.sourceforge.net>.

[9] J.-H. Gao, and S.-H. Yee, "Iterative temporal clustering analysis for the detection of multiple response peaks in fMRI", *Magnetic Resonance Imaging*, Vol. 21, pp. 51-53, 2003.

[10] P. Jezzard, P.W. Matthews, and S.M. Smith (editors), *Functional MRI an introduction to method*, Oxford University Press, 2001.

[11] D.R.M. Langers, P. van Dijk, E.S. Schoenmaker, and W.H. Backes, "fMRI activation in relation to sound intensity and loudness", *NeuroImage*, Vol. 35, No. 2, pp. 709-718, 2007.

[12] S. Lee, F. Zelaya, L. Reed, M.J. Brammer and S.A. Amiel, "A model-free method for fMRI analysis using temporal clustering and neighbourhood constraint", *12th Annual Meeting of the Organization for Human Brain Mapping*, 2006.

[13] S. Lee, F. Zelaya, M.J. Brammer and S.A. Amiel, "Stimulus Response Detection in fMRI Using Temporal Clustering Analysis, Digital Filters and a Two-Dimensional Neighbourhood Test", *Proceedings of the International Computer Symposium, Medical and Bio Informatics*, Vol. 3, pp. 1302-1307, Taipei, Taiwan, 2006.

[14] S. Lee, F. Zelaya, M.J. Brammer and S.A. Amiel, "Stimulus Response Detection in fMRI Using Digital Filters, Temporal Clustering Analysis and a Three-Dimensional Selection Criterion", *Proceedings of the Fifteenth European Signal Processing Conference (EUSIPCO)*, Poznan, Poland.

[15] Y. Liu, J.-H. Gao, H.-L. Liu and P.T. Fox, "The temporal response of the brain after eating revealed by functional MRI", *Nature*, Vol. 405, pp. 1058-1062, 2000.

[16] Matlab, Signal Processing Toolbox, The Mathworks, Inc.

[17] M. McKeown, and T. Sejnowski, "Independent component analysis of fMRI data: examining the assumptions", *Human Brain Mapping*, Vol. 5, pp. 368-372, 1998.

Data	Time bin with the highest number of detected voxels	Time bin with the second highest number of detected voxels
VIS1	¹ 70-80 V	200-210
VIS2	80-90	280-290
VIS3	230-240	⁵ 70-80 V
VIS3	220-230	260-270
VIS-AUD	0-10	280-290
VIS-MOT1	¹¹ 70-80 V	¹³ 250-260 M
VIS-MOT2	¹⁵ 70-80 V	130-140
VIS-MOT3	180-190	170-180
Data	Time bin with the third highest number of detected voxels	Time bin with the fourth highest number of detected voxels
VIS1	80-90	60-70
VIS2	30-40	³ 70-80 V
VIS3	130-140	170-180
VIS3	230-240	290-300
VIS-AUD	⁷ 220-230 A	⁹ 70-80 V
VIS-MOT1	100-110	30-40
VIS-MOT2	140-150	210-220
VIS-MOT3	¹⁷ 250-260 M	170-180

Table 1: The time in (in seconds) and spatial information detected for eight sets of fMRI data using the proposed method. **A**, **M** and **V** indicate that the voxels contributed to the detected time bins are in the areas typically found in auditory, motor and visual sensory experiments respectively. The superscript is the figure number for the corresponding activation map.

[18] S.K. Mitra, *Digital Signal Processing a computer-based approach*, McGraw-Hill International Editions, Electrical Engineering Series, 1998.

[19] S.M. Smith, "Fast robust automated brain extraction", *Human Brain Mapping*, Vol. 17, No. 3, pp. 143-155, 2002.

[20] S.-H. Yee and J.-H. Gao, "Improved detection of time windows of brain responses in fMRI using modified temporal clustering analysis", *Magnetic Resonance Imaging*, Vol. 20, pp. 17-26, 2002.

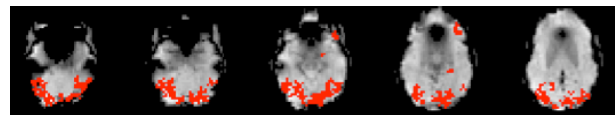


Figure 1: VIS1: the time bin with the highest number of detected voxels was 70-80s and the voxels detected were in the primary and extrastriate visual areas.

Data	Time bin with the highest number of detected voxels	Time bin with the second highest number of detected voxels
VIS1	¹⁹ 70-80 V	150-160
VIS2	80-90	280-290
VIS3	230-240	130-140
VIS3	220-230	260-270
VIS-AUD	0-10	280-290
VIS-MOT1	²⁰ 70-80	250-260 M
VIS-MOT2	130-140	70-80 V
VIS-MOT3	180-190	170-180
Data	Time bin with the third highest number of detected voxels	Time bin with the fourth highest number of detected voxels
VIS1	60-70	280-290
VIS2	30-40	70-80 V
VIS3	70-80 V	170-180
VIS3	230-240	290-300
VIS-AUD	230-240	220-230 A
VIS-MOT1	100-110	60-70
VIS-MOT2	40-50	140-150
VIS-MOT3	250-260 M	350-360

Table 2: The time in (in seconds) and spatial information detected for eight sets of fMRI data without the proposed selection criterion. **A**, **M** and **V** indicate that the voxels contributed to the detected time bins are in the areas typically found in auditory, motor and visual sensory experiments respectively.

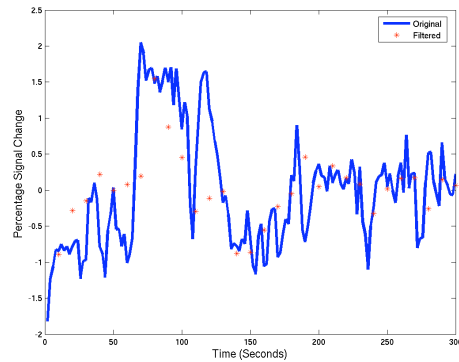


Figure 4: VIS2: the original and filtered fMRI time series extracted from the detected voxels in Fig. 3.

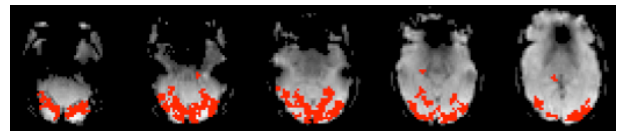


Figure 5: VIS3: the time bin with the second highest number of detected voxels was 70-80s and the voxels detected were in the primary and extrastriate visual areas.

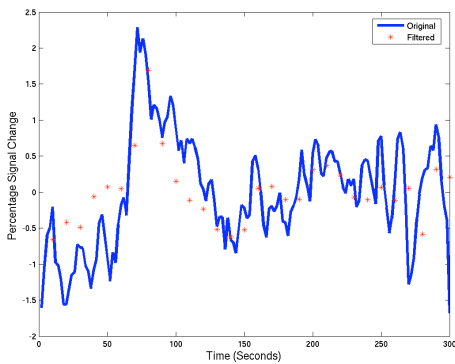


Figure 2: VIS1: the original and filtered fMRI time series extracted from the detected voxels in Fig. 1.

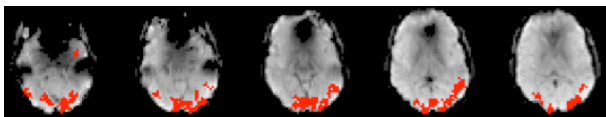


Figure 3: VIS2: the time bin with the fourth highest number of detected voxels was 70-80s and the voxels detected were in the primary and extrastriate visual areas.

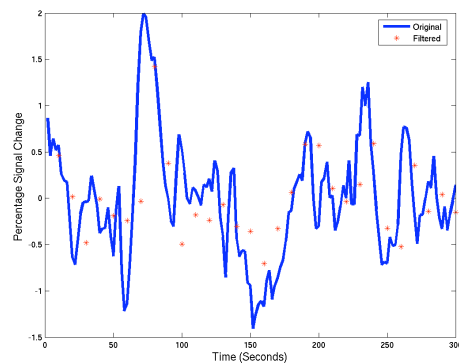


Figure 6: VIS3: the original and filtered fMRI time series extracted from the detected voxels in Fig. 5.

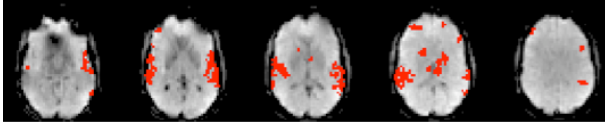


Figure 7: VIS-AUD: the time bin with the third highest number of detected voxels was 220-230s and the voxels detected were in the auditory cortex area.

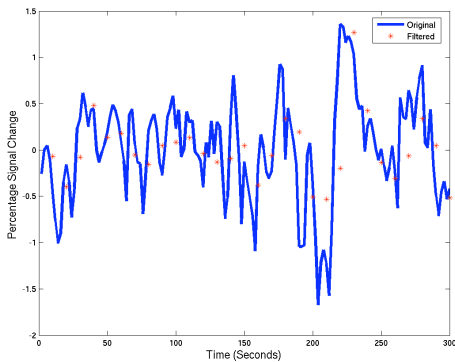


Figure 8: VIS-AUD: the original and filtered fMRI time series extracted from the detected voxels in Fig. 7.

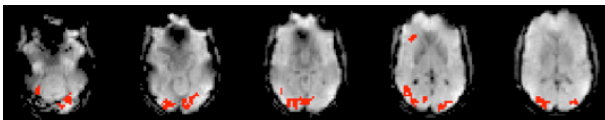


Figure 9: VIS-AUD: the time bin with the fourth highest number of detected voxels was 70-80s and the voxels detected were in the primary and extrastriate visual areas.

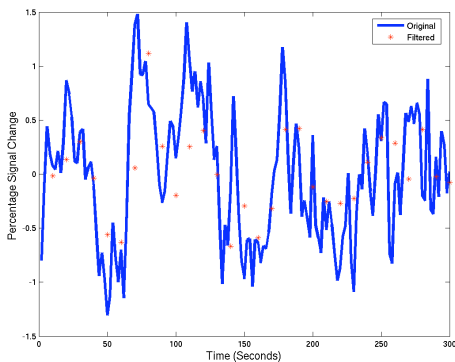


Figure 10: VIS-AUD: the original and filtered fMRI time series extracted from the detected voxels in Fig. 9.

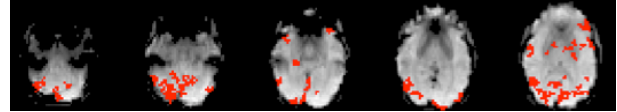


Figure 11: VIS-MOT1: the time bin with the highest number of detected voxels was 70-80s and the voxels detected were in the primary and extrastriate visual areas.

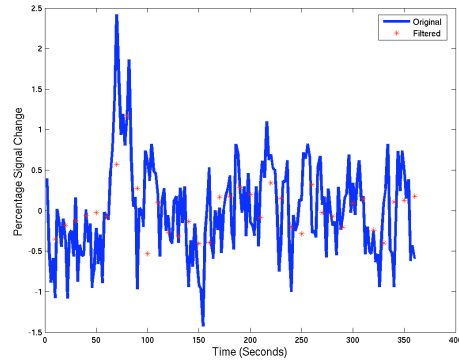


Figure 12: VIS-MOT1: the original and filtered fMRI time series extracted from the detected voxels in Fig. 11.

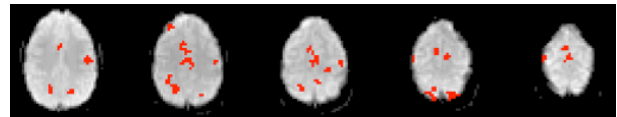


Figure 13: VIS-MOT1: the time bin with the second highest number of detected voxels was 250-260s and the voxels detected were in the motor areas.

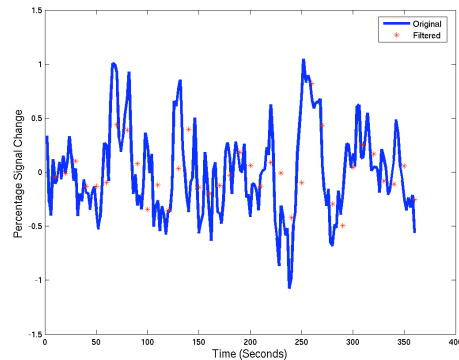


Figure 14: VIS-MOT1: the original and filtered fMRI time series extracted from the detected voxels in Fig. 13.

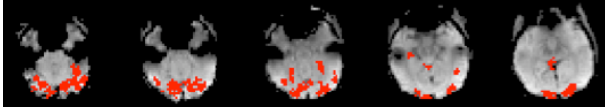


Figure 15: VIS-MOT2: the time bin with the highest number of detected voxels was 70-80s and the voxels detected were in the primary and extrastriate visual areas.

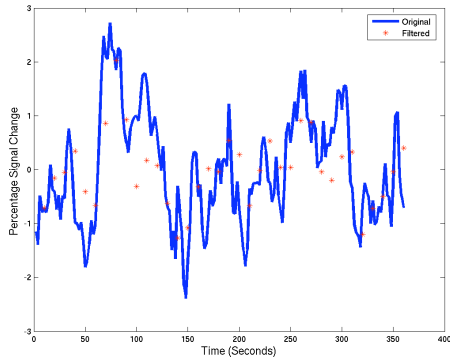


Figure 16: VIS-MOT2: the original and filtered fMRI time series extracted from the detected voxels in Fig. 15.

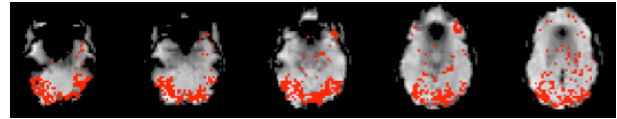


Figure 19: VIS1: the detected voxels at time bin 70-80s when the selection criterion was not applied.

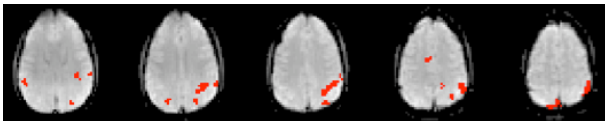


Figure 17: VIS-MOT3: the time bin with the third highest number of detected voxels was 250-260s and the voxels detected were in the motor areas.

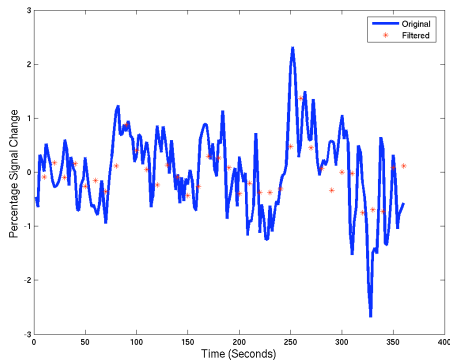


Figure 18: VIS-MOT3: the original and filtered fMRI time series extracted from the detected voxels in Fig. 17.

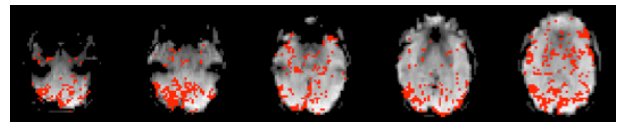


Figure 20: VIS-MOT1: the detected voxels at time bin 70-80s when the selection criterion was not applied.